Density functional investigation of the interaction of acetone with small gold clusters

Ghazal S. Shafai
Department of Physics, University of Pune, Pune 411 007, India

Sharan Shetty and Sailaja Krishnamurty
Centre for Modeling and Simulation, University of Pune, Pune 411 007, India

Vaishali Shah
Institute of Bioinformatics and Biotechnology, University of Pune, Pune 411 007, India

D. G. Kanhere
Department of Physics, University of Pune, Pune 411 007, India and Centre for Modeling and Simulation, University of Pune, Pune 411 007, India

(Received 16 February 2006; accepted 27 November 2006; published online 3 January 2007)

The structural evolution of Au_n ($n=2$, 3, 5, 7, 9, and 13) clusters and the adsorption of organic molecules such as acetone, acetaldehyde, and diethyl ketone on these clusters are studied using a density functional method. The detailed study of the adsorption of acetone on the Au_n clusters reveals two main points. (1) The acetone molecule interacts with one gold atom of the gold clusters via the carbonyl oxygen. (2) This interaction is mediated through back donation mainly from the *spd*-hybridized orbitals of the interacting gold atom to the oxygen atom of the acetone molecule. In addition, a hydrogen bond is observed between a hydrogen atom of the methyl group and another gold atom (not involved in the bonding with carbonyl oxygen). Interestingly, the authors notice that the geometries of Au_9 and Au_{13} undergo a significant flattening due to the adsorption of an acetone molecule. They have also investigated the role of the alkyl chain attached to the carbonyl group in the adsorption process by analyzing the interaction of Au_{13} with acetaldehyde and diethyl ketone.
 [DOI: 10.1063/1.2424458]

I. INTRODUCTION

Conjugated gold nanoparticles are of fundamental interest because of their importance in the self-assembly process to develop potential miniature devices. Several recent reports have been focused on their applications in catalysis, molecular electronics, and DNA sequencing as well as in microscopy markers.[1] The gold nanoparticles, being nontoxic and highly biocompatible, are attractive candidates for therapeutic drug delivery vehicles.[2] Research interest in conjugated gold nanoparticles is also fueled by the realization that their optical, electronic, and catalytic properties characteristically depend on the conjugating molecules that form complexes with the gold nanoparticles.[3,4] This has given impetus to the research efforts directed towards developing different protocols for synthesizing gold nanoparticles of various sizes in aqueous and nonpolar organic solvents.[5]

In the past decade, several theoretical studies have been carried out to understand the structural evolution of gold clusters and their electronic properties. The primary interest has been in investigating the nature of the two dimensional (2D) to three dimensional (3D) structural transition in these clusters.[6–9] This is due to the correlation between the catalytic activity and the shape and dimension of these clusters.[10] Häkkinen and Landman predicted that the occurrence of the 2D to 3D transition is at $n>8$ (n is the number of atoms).[11] Similarly, Olson *et al.* reported that the transition takes place between $n=6$ and 8.[7] Interestingly, it has been proposed that the transition is driven by the *sd* hybridization of the 5*d* and 6*s* orbitals.[11,12]

Besides the structural properties, the catalytic properties of gold clusters have also been of considerable interest. In this context, several studies on the adsorption of O_2 and CO on the Au clusters have been carried out.[10,13–15] Yoon *et al.* have shown that the adsorption of O_2 is more favorable in the case of Au_3 than in Au_n clusters with $n\geqslant 4$.[16] They also predicted that the dissociation of O_2 on Au_n ($n\geqslant 4$) clusters results in a considerable structural distortion of the host clusters. Their study showed that there is a charge transfer from the gold cluster to the O_2 molecule. Ding *et al.* have demonstrated that the odd-numbered neutral clusters have larger adsorption energies than the even-numbered ones.[17] Interestingly, they showed that Au_3 can adsorb two O_2 molecules in contrast to the behavior exhibited by the Au_5 cluster, where only one molecule is adsorbed. Fielicke *et al.* showed that the adsorption of CO on gold clusters can distort their geometry.[18]

Rousseau and Marx have used an *ab initio* molecular dynamics technique to analyze the interaction of a methanol molecule with neutral and cationic Au_n ($n=1-15$) clusters.[19] Interestingly, they showed that the C–O bond in methanol stretches upon adsorbing on the gold clusters. Consequently, positively charged centers are formed on the adsorption sites. Their investigation also revealed the importance of the local

coordination of the adsorption site. Majumder *et al.* have examined the nature of the interaction of thiol with the gold clusters and have proposed that the interaction of the S atom in thiol with the Au site is due to back bonding.[20] Similar back bonding has also been observed by Yoon *et al.* during the catalyzed oxidation of CO on MgO-supported Au_8 clusters.[21] They gave experimental and theoretical evidences for the stretching of the C═O bond and the formation of the back bond.

Recently, several attempts have been made to comprehend the interaction of larger molecules such as DNA bases and other organic systems with gold clusters. Kryachko and Remacle[22] have shown that the adsorption of DNA base pairs on the neutral gold clusters is stabilized through the formation of a chemical bond between either oxygen and gold or nitrogen and gold. In addition, an unconventional Au–H bond is also observed. It may be mentioned that most of the work concerning adsorption of molecules onto the gold clusters is focused on structural changes. A detailed investigation of the changes in the electronic structure and the nature of bonding in these complexes is lacking.

Motivation for the present theoretical investigation is provided by a recent experimental work by Shiv Shankar *et al.* on the synthesis of gold nanotriangles in the presence of lemongrass extract.[23] They have reported that the aldehydes/ketones present in the lemon grass extract account for the flattening of the gold nanoparticles and result in formation of a "fluidlike" surface. Interestingly, similar results were observed in presence of acetone. From their experimental findings, they conjectured that this may be due to the strong interaction of these organic molecules with the gold surface. However, a detailed understanding of this interaction is missing. To our knowledge, no work related to the strength and nature of interaction of aldehydes/ketones with gold nanoparticles has been reported. Hence, in the present work we thoroughly investigate the structural, electronic, and bonding properties of Au_n-acetone complexes (n=2, 3, 5, 7, 9, and 13). In order to understand the effect of the alkyl chain attached to the adsorbing molecule, we have also studied the interaction of acetaldehyde and diethyl ketone with Au_{13}.

II. COMPUTATIONAL DETAILS

All the calculations have been performed using the density functional method[24] within the local density approximation (LDA) as implemented in the VASP.[25] The wave functions were expanded in a plane wave basis with a kinetic energy cutoff of 29.10 Ry. An advantage of using plane waves is that a basis set of this type does not tend to yield significant basis set superposition error, which otherwise would make the calculated energy difference between a complex and its constituent species unreliable. All the core-valence interactions were described by Vanderbilt's ultrasoft pseudopotentials.[26]

The initial configurations of the pure gold clusters were generated by a basin-hopping algorithm,[27] using a parameterized Gupta potential.[28] We have also used a constant-temperature molecular dynamics run at 1200 K (with a simulation time of 90 ps) to generate several other initial configurations. For each of the larger clusters ($n \geqslant 7$), between 100 and 150 geometries were optimized. The geometries were considered to be converged when the forces on each atom were less than 10^{-3} eV/Å. The self-consistent-field calculations were carried out with a convergence in the total energy of the order of 10^{-4} eV. A similar exercise is carried out to obtain the minimum energy configurations of the gold-acetone complexes. Several initial geometries were generated by placing acetone with different orientations on the nonequivalent gold atoms of pure gold clusters. In order to confirm the resulting minimum energy geometries, these clusters were reheated and reoptimized. The electronic and structural rearrangements in the gold clusters after adsorption of acetone were then analyzed. The same approach was followed for the Au_{13}-diethyl ketone and Au_{13}-acetaldehyde complexes.

We have also computed the interaction energy (IE) of the organic molecules, viz., acetone, diethyl ketone, and acetaldehyde, with the Au_n cluster as

$$\mathrm{IE} = E_{\mathrm{Au\ cluster}} + E_{\mathrm{organic\ molecule}} - E_{\mathrm{complex}}.$$

All the energies on the right hand side refer to the total (internal) energies. It should be noted that the total energy convergence is dependent on the energy cutoff used for the plane wave basis. The energy cutoff here has been chosen so as to yield the total energy convergence of 10^{-4} eV for separated, as well as interacting systems. We have verified that the interaction energy is stable with respect to the change in the energy cutoff.

We have analyzed the nature of bonding by using angular momentum and site projected contributions to the total electron density and the frontier orbitals. It is also instructive to examine the difference electron density ($\Delta\rho$) to bring out the changes in the electron density on formation of the gold-acetone complex. $\Delta\rho$ is defined as

$$\Delta\rho = \rho_{\mathrm{complex}} - \rho_{\mathrm{Au\ cluster}} - \rho_{\mathrm{organic\ molecule}},$$

where ρ is the electron density.

III. RESULTS AND DISCUSSION

A. The geometries, energetics, and the electronic properties of gold clusters

Most of the earlier theoretical studies on gold clusters have primarily focused on the structural evolution of Au_n clusters in the range of n=2–20.[6–8] In the present work, we revisit the structural properties of the neutral Au_n (n=2, 3, 5, 6, 7, 8, 9, and 13) clusters before investigating the interaction of odd-numbered Au_n (n=3, 5, 7, 9, and 13) clusters with organic molecules. In the case of Au_2, the calculated Au–Au bond length is 2.47 Å and is in excellent agreement with the experimentally reported value.[29,30] In Fig. 1, we present the ground state geometry of Au_n (n=3, 5, 6, 7, 8, 9, and 13) along with some isomers of Au_{13}.

The lowest energy geometry of Au_3 is an equilateral triangle (D_{3h} symmetry) with Au–Au bond lengths of 2.60 Å (Fig. 1). The other low lying isomers for this cluster are the obtuse triangle and the linear chain (figures not shown). All the three configurations lie within the energy range of

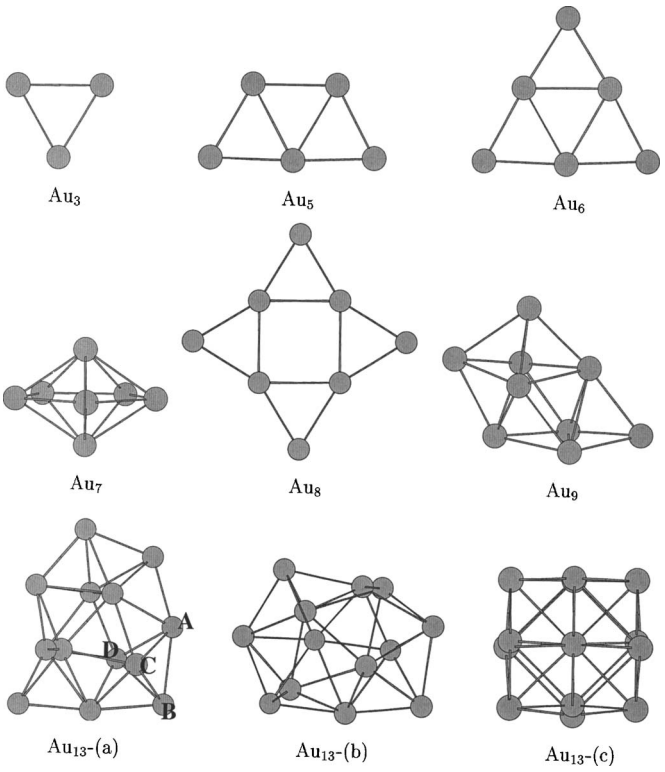

FIG. 1. Ground-state structures of gold clusters and some isomers of Au_{13}.

0.14 eV. Au_5 clearly reflects cluster growth based on the lowest energy Au_3 configuration (with two caps on two edges of the equilateral triangle) and has C_{2v} symmetry.[6–8] All the other low-lying isomers (figures not shown) of Au_5 are almost 0.7 eV higher in energy as compared to the ground state geometry. We also present the geometries of Au_6 and Au_8 clusters, since the 2D to 3D transition is expected to occur in this size range.[7] In agreement with the earlier results, the ground state geometry of Au_6 (Fig. 1) is an equilateral triangle embedded in a bigger one. There are two nearly degenerate structures (within 0.02 eV) for Au_7. The lower energy configuration is a pentagonal bipyramid (Fig. 1) and the next higher energy isomer has a planar configuration (figure not shown). In order to probe the possibility of a structural transition from the 3D to 2D configuration at room temperature, we carried out a limited 10 ps constant temperature molecular dynamics run at 300 K with the 3D structure as the starting configuration. The 3D structure was not found to visit the 2D structure during the run. We also investigated the interaction of acetone with both of these structures.

The present LDA calculation indicates that the planar configuration (see Fig. 1) and 3D configuration (figure not shown) of Au_8 are nearly degenerate with planar configuration being lower in energy by 0.06 eV. Thus, we find planar and nonplanar configurations to be nearly degenerate for Au_7 and Au_8. Therefore, we infer that the transition from 2D to 3D in gold clusters occurs between Au_6 and Au_8. This result is in agreement with the earlier work of Olson *et al.*[7]

The ground state geometry of Au_9 is a bicapped pentagonal bipyramid (Fig. 1). It is interesting to note that the energy difference between the ground state geometry (which is a 3D configuration) and the next lowest lying isomer (a planar configuration) is 0.36 eV. This difference is substantially more than that of Au_n (n=6, 7, and 8). The lowest energy configuration of Au_{13} is a hexagonal bipyramid interpenetrating with a capped pentagonal bipyramid (C_{2v}) [Fig. 1, Au_{13}(a)]. We would like to note that this structure is quite different from the earlier reported ground state geometries for this cluster.[6,31] Our ground state geometry is lower in energy by 0.08 eV in comparison with the previously reported ground state structure [Fig. 1, Au_{13}(b)], which has been described as an amorphous geometry.[31] The other isomer of Au_{13} is shown in Fig. 1 as Au_{13}(c).

TABLE I. Binding energy (eV/atom), average Au–Au bond length (Å), and HOMO-LUMO gap (eV) of the clusters studied.

System	BE/atom (eV)	Average Au–Au bond length (Å)	HOMO-LUMO energy gap (eV)
Au_3	1.67	2.60	2.85
Au_5	2.32	2.63	1.48
Au_7	2.57	2.70	1.02
Au_9	2.74	2.72	0.97
Au_{13}	2.98	2.74	0.77

The binding energy per atom (BE/atom), average Au–Au bond length, and the energy gap between the highest occupied molecular orbital (HOMO) and lowest unoccupied molecular orbital (LUMO) as a function of the size of the cluster are reported in Table I. The BE/atom increases monotonically as a function of the size of the cluster. It is also noted that the Au–Au bond lengths of Au_3 are considerably shorter and closer to the covalent Au–Au bond length (2.47 Å). As the size of the cluster grows, the average Au–Au bond length increases towards the average metallic (bulk) Au–Au bond length (2.88 Å). In addition, the coordination number of the gold atoms also increases. This indicates that as the size of the cluster grows, each gold atom forms a larger number of bonds. Table I also clearly shows that there is a decrease in the HOMO-LUMO energy gap with an increase in the size of the clusters. This is associated with an increase in the metallic character of gold cluster as the number of atoms is increased.

B. The geometries, energetics, and the electronic properties of gold-acetone complexes

In order to locate the most reactive site of the acetone molecule during its interaction with a single gold atom and with a gold dimer, we carried out the total energy minimization starting with various possible connectivities of these complexes. The highest binding energy is obtained when the gold atom or gold dimer interacts with the carbonyl oxygen, indicating this to be the most favored site of interaction. For example, the IEs for a single gold atom with the oxygen and hydrogen sites are 0.70 and 0.37 eV, respectively. When a single gold atom or dimer is placed near the carbon atom, it moves away so as to form a bond with carbonyl oxygen during the process of optimization.

For each of the Au_n clusters, several initial configurations are optimized (8–30 depending on the size) to find the

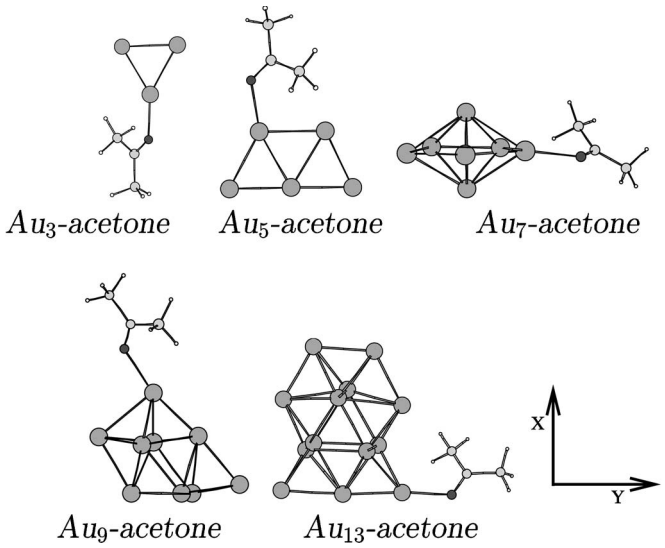

FIG. 2. Ground-state geometries of Au_n-acetone complexes. Coordinate axes are shown for reference; the z axis is perpendicular to the plane.

minimum energy configuration of the complex. The initial configurations were formed by placing acetone with different orientations adjacent to the nonequivalent gold atoms of pure gold clusters. It is clear that in all these complexes, acetone interacts with the gold clusters via its most reactive site, which is the oxygen atom. The lowest energy configuration of each gold-acetone complex is shown in Fig. 2.

In Figs. 3(a)–3(d), we display the variation in the interaction energy, the C═O bond length, the Au–O bond length, and the Au–H bond length as a function of the size of the cluster. We note that the interaction energy of acetone with Au_2 is 1.37 eV. It can be seen that upon adsorption, the Au–Au bond length does not show a significant change, while the C═O bond length increases from 1.21 to 1.25 Å, and the C–C–C bond angle in acetone increases from 116.00° to 120.00°. The increase in the C═O bond length in acetone is indicative of some charge transfer from the Au atom to the O atom.

It is seen that the bond between the carbonyl oxygen and Au_n (n=3 and 5) is within the plane of the clusters. An examination of all the geometries in Fig. 2 shows that after interaction, one of the CH_3 groups in acetone is reoriented. This rearrangement allows one hydrogen atom of the CH_3 group to form a hydrogen bond with one of the gold atoms. This kind of hydrogen bond has been observed in the earlier work on the interaction of DNA bases with gold clusters.[22] From Fig. 3(d), it is seen that the lengths of the hydrogen bonds lie in the range of 2.1–2.7 Å. A comparison of Figs. 3(a) and 3(c) clearly indicates that the variation in the IE closely follows the variation in the Au–O bond length, indicating that the dominant contribution to the IE comes from the Au–O bond. It can be seen from Fig. 3(a) that the IE is the highest for Au_3, it is a minimum for Au_7, and it increases thereafter. Thus, the strongest interaction is with Au_3. It may be noted that the interacting atom in this cluster has the smallest coordination number when compared with the interacting atoms in the rest of the clusters. We also observe another interesting correlation between IE and the contribution of the s component in the HOMO. In Table II, we show the s, p, and d components, site projected onto the interacting gold atom before and after interaction. It can be seen that after the interaction, the HOMO is almost purely d type, a result indicating that the charge transfer is almost exclusively coming from the s part of the orbital. Whenever the s contribution is large in the pure gold clusters, the IE is large.

As mentioned above, there are two nearly degenerate 3D and 2D structures for Au_7. We investigated the interaction of both of these structures with acetone. Our results show that the interaction energy in the case of the 2D structure is slightly (10%) higher than that obtained for 3D structure. The other characteristics are found to be very similar.

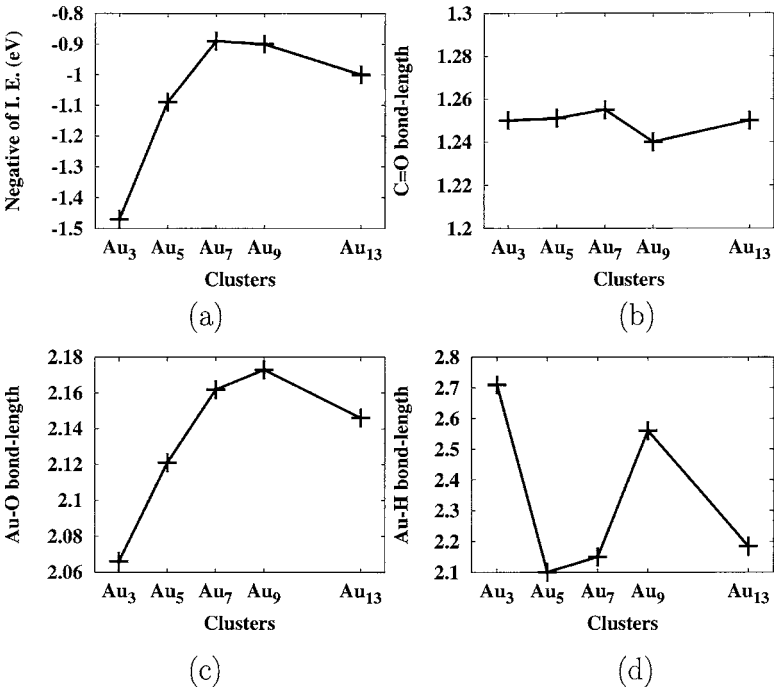

FIG. 3. The variation of (a) interaction energy, (b) C═O bond length, (c) Au–O bond length and (d) Au–H bond length as a function of size of the cluster in the complex.

TABLE II. *s*, *p*, and *d* contributions to the HOMO of the interacting Au atom of gold clusters before and after interaction with acetone.

	Bare gold cluster			Au-acetone complex		
System	*s*	*p*	*d*	*s*	*p*	*d*
Au_2	0.02	0.00	0.97	0.00	0.00	0.99
Au_3	0.70	0.04	0.26	0.00	0.15	0.85
Au_5	0.58	0.10	0.32	0.08	0.03	0.89
Au_7	0.00	0.18	0.81	0.00	0.07	0.90
Au_9	0.00	0.20	0.78	0.07	0.04	0.89
Au_{13}	0.36	0.17	0.48	0.05	0.02	0.92

Finally, we would like to note a significant structural change observed in the case of the 3D geometries when the gold clusters interact with the acetone molecule. We observe a substantial reduction in the shorter dimension (shown as the *z* axis) in these clusters. For example, the change in the relevant bond lengths in the case of Au_9 and Au_{13} are as high as 16% and 17%, respectively (for a detailed discussion on this point, see the next section).

C. Bonding

In this section, we examine the nature of the bonding between the carbonyl oxygen and the gold clusters. To analyze this, we investigated the characteristics of the frontier orbitals of the individual systems as well as those of complexes. The angular momentum decompositions of all the HOMOs, projected on the interacting gold atom, are given in Table II. To understand the charge transfer process, the difference electron density ($\Delta\rho$) of the complexes has been analyzed. In Figs. 4(a) and 4(b), we show the isodensity surfaces of the the HOMO and the LUMO of an isolated acetone molecule. It can be seen that the HOMO and the LUMO are of the *p* type and are perpendicular to each other. In Figs. 5(a) and 5(b), we show the isodensity surfaces of the HOMO for pure Au_3 and the Au_3-acetone complex, and finally in Fig. 5(c), we show the isodensity surfaces for $\Delta\rho$. The dark regions in the figure indicate charge depletion, and light areas represent the regions where charge is gained.

The HOMO of pure Au_3 [Fig. 5(a)] shows *sd*-hybridized orbitals on all three gold atoms, deriving from the $5d^{10}$ and $6s^1$ atomic orbitals. As seen in Table II and Fig. 5(b), the hybridized *sd* orbital on the Au site becomes purely *d* like after interaction due to the loss of its *s* component. This result shows that the charge is transferred from the *s* orbital of Au to the *p* orbital of O atom in acetone. The analysis of

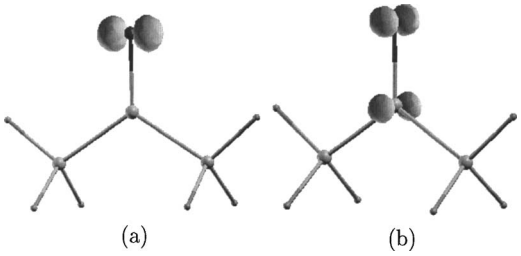

FIG. 4. Isodensity surfaces at one-third of the maximum value of (a) the HOMO of acetone and (b) the LUMO of acetone.

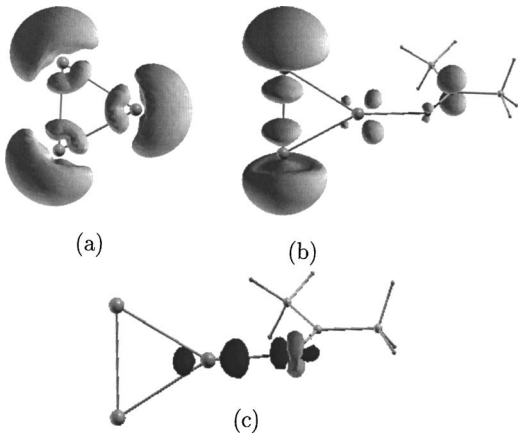

FIG. 5. Isodensity surfaces at one-third of the maximum value of (a) the HOMO of Au_3, (b) the HOMO of Au_3-acetone, and (c) the difference electron density of the Au_3-acetone complex. The dark and light regions in (c) are the charge-depleted and charge-gained regions, respectively.

$\Delta\rho$ shows that charge is also transferred from the HOMO of oxygen to the perpendicular orbital, namely, the LUMO of oxygen. This transfer signifies a back donation of the charge from a localized *sd* orbital to the LUMO of oxygen. This kind of back donation or back bonding has also been observed in the adsorption of CO on gold clusters.[21] As noted above, this leads to the stretching of the C═O bond length from 1.22 Å (free acetone) to 1.25 Å. Such a back bond is also observed in the case of the Au_2-acetone complex.

The isodensity surfaces of the HOMO of pure Au_5, the Au_5-acetone complex, and their $\Delta\rho$ are shown in Figs. 6(a)–6(c), respectively. The analysis of the HOMO shows bond formation between the top two gold atoms depicted in the structure of pure Au_5. It can be seen that the HOMO contains dominantly an *s* component along with lesser *d* and weak *p* components. The orbital components on the remaining three gold atoms have a dominant *d* character (not shown in Table II). After the adsorption of acetone, the interacting

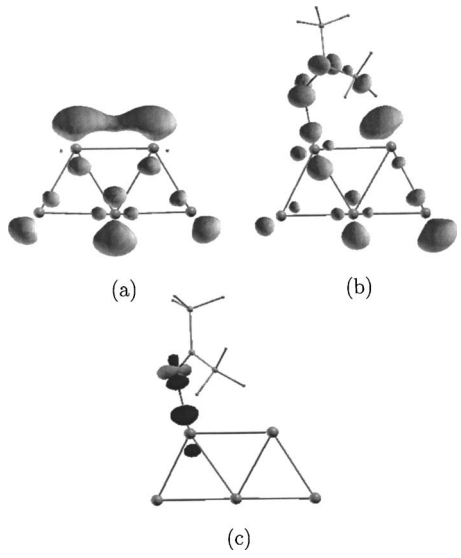

FIG. 6. Isodensity surfaces at one-third of the maximum value of (a) the HOMO of Au_5, (b) the HOMO of Au_5-acetone, and (c) the difference electron density of the Au_5-acetone complex. The dark and light regions in (c) are the charge-depleted and charge-gained regions, respectively.

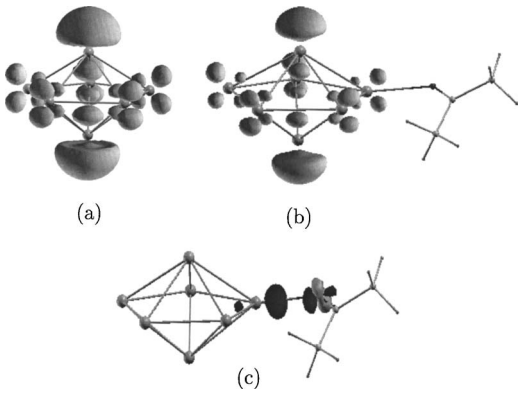

FIG. 7. Isodensity surfaces at one-third of the maximum value of (a) the HOMO of Au_7, (b) the HOMO of Au_7-acetone, and (c) the difference electron density of the Au_7-acetone complex. The dark and light regions in (c) are the charge-depleted and charge-gained regions, respectively.

atom loses its *s* character and forms a back bond similar to that seen in the case of Au_3. Au_7 is the smallest 3D structure investigated, and its structure is the least disturbed after complexation with an acetone molecule. From Table II, it is seen that the HOMO of the pure Au_7 cluster is dominantly *d* in character with a weak *p* component and that there is a charge transfer from the *p* component that accompanies complexation. Figure 7 shows the back bonding in the Au_7-acetone complex, which is similar to that seen in cases of the Au_3-acetone and Au_5-acetone complexes. The interaction leads to about a 4% reduction in the height (along the *z* dimension) of this cluster.

The nature of the bonding in the Au_9-acetone complex follows a similar pattern to that found for the Au_7-acetone complex. This similarity explains why the IE values of Au_7 and Au_9 [Fig. 3(a)] are almost the same.

Au_{13} is the largest cluster that we have studied. The HOMOs of pure Au_{13} and the Au_{13}-acetone complex are shown in Figs. 8(a) and 8(b), respectively. It is interesting to note that an analysis of the HOMO of pure Au_{13} shows formation of a bond between the interacting atom (marked A) and its neighbor (marked B), similar to that observed in Au_5. All the other orbitals localized on the gold atoms are *spd* hybridized, with a dominantly *d* character. After interaction, the Au_{13} cluster becomes symmetric, one of the Au–Au bonds (between A and B) is broken, and the nature of the HOMO changes to dominantly *d* type on the interacting site. Back bonding is also seen along with charge transfer from a gold atom to carbonyl oxygen in Fig. 8(c).

Now we discuss the possible reasons for the significant structural rearrangements in Au_{13} that have been noted earlier. We offer an explanation on the basis of the observed changes in the molecular orbitals (MOs) and in the nature of the bonding due to the interaction with acetone. In Fig. 9(a), we show the isodensity surfaces of the MO that demonstrates the formation of a three-centered bond in pure Au_{13}, and in Fig. 9(b), we show the isodensity surfaces of the relevant MO (24th MO, occurring in the middle of the "band"). It may be noted that there are four atoms which are involved in this rearrangement [marked in Fig. 1, Au_{13}(a) and Fig. 9]. Atom A is the interacting site: atoms B, C, and D are the nearest neighbors of atom A, and they are all at a distance of

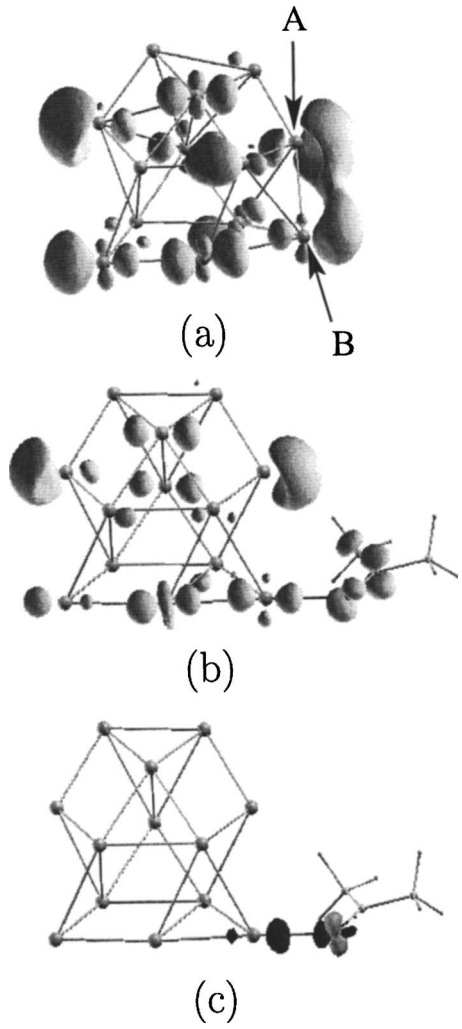

FIG. 8. Isodensity surfaces at one-third of the maximum value of (a) the HOMO of Au_{13}, (b) the HOMO of Au_{13}-acetone, and (c) the difference electron density of the Au_{13}-acetone complex. The dark and light regions in (c) are the charge-depleted and charge-gained regions, respectively.

2.7 Å. As noted earlier, atoms A and B in pure Au_{13} form a bond due to the overlap of *sd*-hybridized orbitals [see Fig. 8(a)]. In addition, atoms A, B, and C form a three-centered bond [see Fig. 9(a)] as a result of the overlap of their localized *d* orbitals (d_{xz}, d_{yz}, and d_{xy}, respectively). It may be noted that atom D does not form a bond with atom C, and the distance between them is 3.41 Å. As a consequence of the interaction with acetone, the interacting site A loses the *s*-type contribution to its charge distribution, and therefore it

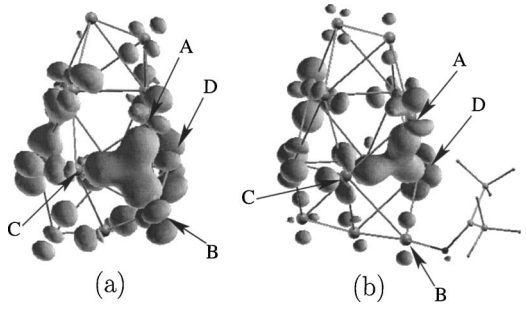

FIG. 9. Isodensity surfaces at one-third of the maximum value of (a) the third band in pure Au_{13} and (b) the 24th band in the complex.

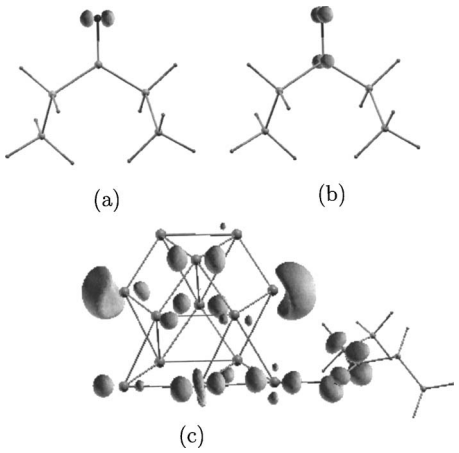

FIG. 10. Isodensity surfaces at one-third of the maximum value of (a) the HOMO of diethyl ketone, (b) the LUMO of diethyl ketone, and (c) the HOMO of the diethyl ketone-Au_{13} complex.

is not viable to have a bond between atoms A and B. As a result, the bond between A and B is broken, and the atoms move away to a distance of 3.76 Å. However, the energy of the Au_{13}-acetone complex is lowered by the formation of a three-center bond between B, C, and D from the overlap of localized *d* orbitals [see Fig. 9(b)].

D. Adsorption of diethyl ketone and acetaldehyde on Au_{13}

Shiv Shankar *et al.*[23] have reported the presence of aldehydes and ketones in the lemon grass extract used in the self assembly of gold nanoparticles. Like acetone, aldehydes and other ketones present in the extract are also believed to play a role in the "flattening" of gold nanoparticles. Hence, in addition to the interaction of the smallest ketone (acetone), we have also investigated the interactions of diethyl ketone and acetaldehyde with Au_{13}.

We calculated and compared the IEs of the diethyl ketone and acetaldehyde complexes formed with the Au_{13} cluster, and they are, respectively, 0.05 eV higher and 0.06 eV lower than the value obtained for the Au_{13}-acetone complex. Thus, the addition of a longer chain or a change in the methyl group does not seriously affect the interaction energy. Figure 10(a) shows the HOMO, Fig. 10(b) shows the LUMO of the diethyl ketone molecule, and Fig. 10(c) shows the HOMO of the Au_{13}-diethyl ketone complex. It can be seen that the HOMO and LUMO of diethyl ketone are similar to those of the acetone molecule. Moreover, the HOMO and the LUMO isodensity surfaces of the acetaldehyde (not shown) also show a similar shape. This similarity clearly suggests that the mode of interaction of diethyl ketone and acetaldehyde with Au_{13} would be similar to that of acetone. As we do not expect the nature of the bonding to be different, we allow diethyl ketone and acetaldehyde to interact with the gold cluster at the atomic site which is energetically favored by acetone. We investigated different orientations of the diethyl ketone and acetaldehyde moieties to find the lowest energy configuration of the complexes. The energetically preferred orientation of diethyl ketone complexed with Au_{13} is seen in Fig. 10(c). An examination of the isodensity surfaces of the

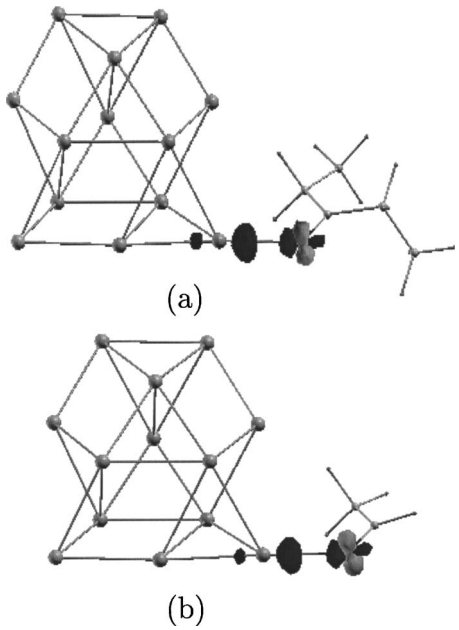

FIG. 11. Isodensity surfaces at one-third of the maximum value of (a) the difference electron density of the diethyl ketone-Au_{13} complex and (b) the difference electron density of the acetaldehyde-Au_{13} complex. The dark and light regions are the charge-depleted and charge-gained regions, respectively.

HOMO and $\Delta\rho$ indicates that the nature of the interaction is quite similar to what is seen in the case of the Au_{13}-acetone complex. In the case of the Au_{13}-acetaldehyde complex, similar behavior is observed. Again, a change in the geometry of the gold cluster is observed upon adsorption of the organic species. In both the cases, Au_{13}-diethyl ketone and Au_{13}-acetaldehyde, the nature of the HOMO of the complex is found to be similar to what is seen in the case of the Au_{13}-acetone complex. Therefore, we show only the $\Delta\rho$ isodensity surfaces for the Au_{13}-diethyl ketone and Au_{13}-acetaldehyde complexes in Figs. 11(a) and 11(b), respectively. We can clearly see that back bonds similar to those found in the Au_{13}-acetone complex are formed. Thus, from our study it is reasonable to expect that aldehydes and ketones in general will show similar behavior when interacting with small gold clusters.

IV. CONCLUSION

The present work reports an *ab initio* density functional investigation of the adsorption of acetone, diethyl ketone, and acetaldehyde on small gold clusters. Furthermore, our calculations on the pure gold clusters show that the 2D to 3D structural transition occurs between Au_6 and Au_8, a result which is in agreement with earlier reports.

Our results on the adsorption of acetone show that the interaction energy of acetone with gold clusters ranges from 0.9 to 1.5 eV, with Au_3 showing the highest interaction energy. There is a strong correlation between the IE and the contribution of the *s* component to the electron density on the interacting gold atom. Our analysis of the electronic structure reveals that the gold clusters interact with acetone by forming a back bond between the hybridized *spd* orbital of the interacting gold site and the *p* orbital of the carbonyl

oxygen. In all these clusters, we observe a charge transfer from the occupied orbital of the interacting gold atom and the *p* orbital of oxygen to the unoccupied *p* orbital of the oxygen atom of acetone, resulting in a back bond. In addition, we also observe a hydrogen bond between a gold atom in the cluster and a hydrogen atom of acetone, indicating multiple interactions between the gold cluster and the adsorbed acetone molecule. In a large cluster such as Au_{13}, there is a significant structural change which is attributed to *s*-type charge transfer.

Our investigation reveals that the nature of the interaction of diethyl ketone and acetaldehyde with the gold clusters is similar to that observed in the case of acetone: an IE of the order of 1 eV and a reduction in the vertical bond lengths by about 17%.

ACKNOWLEDGMENTS

The authors would like to acknowledge Inter-University Centre for Astronomy and Astrophysics (IUCAA), IFCPAR-CEFIPRA (Project No. 3104-2), and the Centre for Development of Advanced Computing (C-DAC) for partial computing support. They are thankful to Murali Sastry for valuable discussions on the experimental results. One of the authors (V.S.) would like to acknowledge the hospitality of the Bioinformatics Centre during the course of this work.

[1] R. Jin, Y. Cao, C. A. Mirkin, K. L. Kelly, G. C. Schatz, and J. G. Zheng, Science **294**, 1901 (2001); C. A. Mirkin, R. L. Letsinger, R. C. Mucic, and J. J. Storhoff, Nature (London) **382**, 607 (1996); E. Hao, G. C. Schatz, and J. T. Hupp, J. Fluoresc. **14**, 331 (2004); S. J. Oldenberg, J. B. Jackson, S. L. Westcott, and N. J. Halas, Appl. Phys. Lett. **75**, 2897 (1999); M. B. Cortie and E. Van der Lingen, Mater. Forum **26**, 1 (2002); M. Haruta, T. Kobayashi, H. Sano, and M. Yamada, Chem. Lett. **2**, 405 (1987).
[2] J. L. West and N. J. Halas, Annu. Rev. Biomed. Eng. **5**, 285 (2003).
[3] T. H. Lee and K. M. Ervin, J. Phys. Chem. **98**, 10023 (1994); I. L. Grazón, K. Michaelian, M. R. Beltrán, P. Ordejón, J. Junquera, D. Sánchez-Portal, E. Artacho, and J. M. Soler, Phys. Rev. Lett. **85**, 5250 (2000).
[4] H. Häkkinen, M. Moseler, and U. Landman, Phys. Rev. Lett. **89**, 033401 (2002).
[5] M. Valden, X. Lai, and D. W. Goodman, Science **281**, 1647 (1998).
[6] S. Gilb, P. Weis, F. Furche, R. Ahlrichs, and M. M. Kappes, J. Chem. Phys. **116**, 4094 (2002); A. V. Walker, J. Chem. Phys. **122**, 094310 (2005); J. Zhao, J. Yang, and J. G. Hou, Phys. Rev. B **67**, 085404 (2003).
[7] R. M. Olson, S. Varganov, M. S. Gordon, H. Metiu, S. Chretien, P. Piecuch, K. Kowalski, S. A. Kucharski, and M. Musial, J. Am. Chem. Soc. **127**, 1049 (2005).
[8] B. S. de Bas, M. J. Ford, and M. B. Cortie, J. Mol. Struct. **686**, 193 (2004).
[9] F. Remacle and E. S. Kryachko, J. Chem. Phys. **122**, 044304 (2005).
[10] G. Mills, M. S. Gordon, and H. Metiu, J. Chem. Phys. **118**, 4198 (2003).
[11] H. Häkkinen and U. Landman, Phys. Rev. B **62**, R2287 (2000).
[12] H. Häkkinen, B. Yoon, U. Landman, X. Li, H.-J. Zhai, and L.-S. Wang, J. Phys. Chem. A **107**, 6168 (2003).
[13] T. Hayashi, K. Tanaka, and M. Haruta, J. Catal. **178**, 566 (1998).
[14] M. Valden, X. Lai, and D. W. Goodman, Science **281**, 1647 (1998); L. M. Molina and B. Hammer, Phys. Rev. Lett. **90**, 206102 (2003); H. Tsunoyama, H. Sakurai, Y. Negishi, and T. Tsukuda, J. Am. Chem. Soc. **127**, 9374 (2005).
[15] M. Haruta, N. Yamada, T. Kobayashi, and S. Lijima, J. Catal. **115**, 301 (1989).
[16] B. Yoon, H. Häkkinen, and U. Landman, J. Phys. Chem. A **107**, 4066 (2003).
[17] X. Ding, Z. Li, J. Yang, J. G. Hou, and Q. Zhu, J. Chem. Phys. **120**, 9594 (2004).
[18] A. Fielicke, G. von Helden, G. Meijer, D. B. Pedersen, B. Simard, and D. M. Rayner, J. Am. Chem. Soc. **127**, 8416 (2005).
[19] R. Rousseau and D. Marx, J. Chem. Phys. **112**, 761 (2000).
[20] C. Majumder, T. M. Briere, H. Mizuseki, and Y. Kawazoe, J. Chem. Phys. **117**, 2819 (2002).
[21] B. Yoon, H. Häkkinen, U. Landman, A. S. Wörz, J.-M. Antonietti, S. Abbet, K. Judai, and U. Heiz, Science **307**, 403 (2005).
[22] E. S. Kryachko and F. Remacle, Nano Lett. **5**, 735 (2005); E. S. Kryachko and F. Remacle, J. Phys. Chem. B **109**, 22746 (2005).
[23] S. Shiv Shankar, A. Rai, B. Ankamwar, A. Singh, A. Ahmad, and M. Sastry, Nat. Mater. **3**, 482 (2004).
[24] M. C. Payne, M. P. Teter, D. C. Allen, T. A. Arias, and J. D. Joannopoulos, Rev. Mod. Phys. **64**, 1045 (1992).
[25] VASP, Vienna *ab initio* simulation package, Technische Universität Wien, 1999; G. Kresse and J. Furthmüller, Phys. Rev. B **54**, 11169 (1996).
[26] D. Vanderbilt, Phys. Rev. B **41**, 7892 (1990).
[27] F. Chuang, Z. Wang, S. Ögüt, R. Chelikowsky, and K. M. Ho, Phys. Rev. B **69**, 165408 (2004).
[28] E. Cleri and V. Rosato, Phys. Rev. B **48**, 22 (1993).
[29] *CRC Handbook of Chemistry and Physics*, 55th ed., edited by R. C. Weast (CRC, Cleveland, OH, 1974).
[30] *American Institute of Physics Handbook* (McGraw-Hill, New York, 1972).
[31] J. Wang, G. Wang, and J. Zhao, Phys. Rev. B **66**, 035418 (2002).